Contents lists available at **CEPM**

Computational Engineering and Physical Modeling

Journal homepage: www.jcepm.com

Wave Propagation through a Submerged Horizontal Plate at the Bottom of a Water Channel

A. Asaiean[1], M. Abedi[2], R.A. Jafari-Talookolaei[3*], M. Attar[4]

1. M.Sc. Student, Department of Mechanical Engineering, Babol Noshirvani University of Technology, Babol, Iran
2. Assistant Professor, Department of Mechanical Engineering, Faculty of Engineering and Technology, University of Mazandaran, Babolsar, Iran
3. Associate Professor, Department of Mechanical Engineering, Babol Noshirvani University of Technology, Babol, Iran
4. Research Associate, Department of Civil, Environmental and Mining Engineering, University of Western Australia, Perth, Australia

Corresponding author: *ramazanali@gmail.com*

https://doi.org/10.22115/CEPM.2020.243377.1123

ARTICLE INFO

Article history:
Received: 11 August 2020
Revised: 23 September 2020
Accepted: 06 October 2020

Keywords:
Submerged horizontal plate;
Water surface waves;
Rectangular plates;
Water channel;
Fluid-structure interaction.

ABSTRACT

Vibrational study of fluid-structure interaction is one of the most widely used cases in engineering. In various industries, the effect of fluid on the structure and vice versa is necessary to investigate such as shipbuilding, ocean energy sources, offshore structures, etc. In this paper, the dynamic behavior of a long rectangular plate located on a viscoelastic bed at the bottom of a narrow channel has been studied in detail. According to earlier studies, the muddy seabed of coasts attenuate the waves. Here we investigate the interaction between the gravity sea waves and the muddy seabed by modeling the seabed as a rectangular plate that located on a viscoelastic foundation which contains springs and dampers. The springs and dampers are attached at the bottom of plate to model the behavior of the muddy seabed. The governing equations of motion have been obtained and a new semi-analytical solution has been presented to solve them. The proposed model is validated against available literatures. Then, the influence of different parameters such as boundary conditions, plate's rigidity and mass, damping ratio, restoring force and different transverse modes on the vibrational behavior of the system has been investigated in detail. The effects of various parameters on the frequency response of the system have been studied in detail.

How to cite this article: Asaeian A, Abedi M, Jafari-Talookolaei R-A, Attar M. Wave propagation through a submerged horizontal plate at the bottom of a water channel. Comput Eng Phys Model 2020;3(4):1–19.
https://doi.org/10.22115/cepm.2020.243377.1123

1. Introduction

According to the research that done by Creel in 2003, about 3 billion people live within a 200 km distance from coastlines, which is forecasted to double in 2025 [1]. This high concentration of population has made significant improvement in industry, urban life and tourism on the coastlines. Therefore, the safety of coastal areas against storm waves and tsunamis are important.

In a study done by Gade [2] in 1958, a phenomenon observed that the sea waves amazingly damped at the coasts with muddy seabed. As shown in Fig. 1, the waves attenuated by overpassing the muddy seabed and accordingly, wave's height decreases gradually [3], Another example of this natural phenomenon could be found on the coast of South India [4]. It should be noted that the attenuation of energy by the muddy seabed has made the southern coast of India, with 2 to 5 meters depth, a safe place for local fishermen against powerful waves.

Fig. 1. Aerial photo of a muddy coast in Brazil [3].

Also, further studies done around the world by silvester [5], Machpherson and Kurup [6] and Sheremet and Stone [7] which verify the Gade's claim. Shermet and Stone [7] reported that the height of the waves decreased up to 70% through the muddy seabed compared to the sandy seabed.

After that, scholars presented different models to study the behavior of muddy seabed. Macpherson [8] analyzed the interaction of a two-layered fluid system that the above layer of fluid is inviscid and the bottom layer is a viscoelastic fluid. It has been claimed that the muddy seabed has elastic and viscous behavior which elastic one causes restoring force and viscous one acts like internal fraction. In addition, Dalrymple and Liu [9] analyzed the two-layer fluid system with assumption of Newtonian viscous fluid for the bottom layer. It has been found an acceptable damping rates of muddy seabed in comparison to the studies done by Gade [2] and Macpherson [8]. Alam et al. [10] also used two-layered fluid system to investigate two dimensional (2D) and three dimensional (3D) model of wave propagation that has been generated by ships and submarines. By comparing the results of nonlinear model and direct simulation, they proved that the calculations have an acceptable accuracy. Another model of muddy seabed has been studied by Liu and Mei [11] in 1993. They modeled the muddy seabed as a Bingham plastic.

The vibration analysis of a thin plate in contact with the fluid has been widely noticed in the literatures. In 2012, Alam [12,13] presented the idea of using a flexible thin plate on the seabed as the carpet wave energy converter (CWEC). He proved that the energy of the surface waves could be absorbed by using an artificial flexible plate on the viscoelastic bed. The viscoelastic

bed contained springs and generators (dampers), which is responsible for elastic and viscous behavior of muddy seabed, respectively. The most important advantage of energy absorbent carpet is its high ability to absorb the sea waves in comparison to other converters, which increases the efficiency of this type of converters. It also provides a safe area for coastline residents and anglers against stormy waves. In 2018, Asaiean et al. [14] assumed the muddy seabed as a flexible plate located at the bottom of the channel and studied the effects of mass and flexural rigidity of the plate which have been neglected in previous studies. It is worth mentioning that only sliding-sliding boundary conditions of the plate can be conducted using the solution methodology presented in [14].

The fluid-structure interaction problems are one of the most important problems in offshore engineering. In recent studies, the interaction of horizontal and vertical plates with gravitational waves has been studied at different depths. In 2001, Sahoo et al. [15] analyzed scattering of surface waves caused by a floating semi-infinite elastic plate with finite depth using Fourier analysis. Mondal and Sahoo [16] studied interaction of gravitational waves with ice sheet covered water surface in three dimensions. The aim of similar studies is to investigate the fluid-structure interaction of wave makers [17], crack in floating ice sheets [18] and wave energy absorbers[12].

In this paper, a 3D model of submerged horizontal plate has been analyzed. The plate is located at the bottom of a channel with different boundary conditions through the channel's width. The governing equations of motion for the system have been obtained and a new solution method has been introduced in this paper to obtain the response. In addition, the effect of boundary conditions, higher modes, mass and flexural rigidity of plate, restoring force and damping ratio of viscoelastic on frequency of system have been investigated.

2. Research significance

In the previous studies, except author's previous publication [14], the submerged horizontal structure has been assumed to be one-dimensional (1D), namely beam located at the bottom of the sea. In addition, the flexural rigidity and the mass of the structure have been neglected. It is clear that the elasticity and mass of the structure should be considered to obtain the more accurate results from the model.

In this paper, the simplification of interaction between gravity waves and submerged horizontal structure is reduced so that the results are more reliable. Therefore, by presenting a more accurate model, it is possible to study other influential factors such as boundary conditions and the material of structure. Another advantage of this study is the presentation of a new solution method to investigate the dynamic response of structure.

3. Methods

As shown in Fig. 2, the submerged horizontal plate has infinite length, finite width b and constant thickness d, and it is placed at the depth h on the channel bed. The linear free surface incident waves move along the positive direction of the x-axis with the wavenumber $k = 2\pi/\lambda$

(where λ is the wavelength) while the thin flexible plate is connected to the viscoelastic foundation at the channel bed. This viscoelastic foundation is composed of normal springs and generators (modeled as dash-pot dampers) which act linearly in the z-direction.

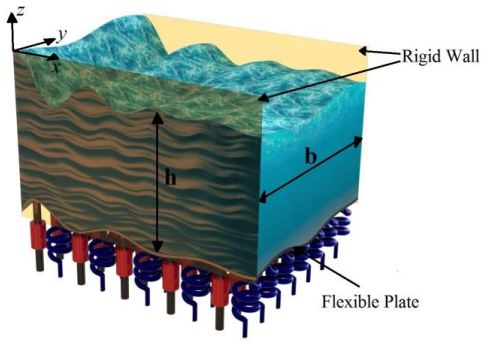

Fig. 2. Schematic view of the system considered in this study.

3.1. Governing equations for the problem of wave-structure interaction

For the fluid domain $-\infty < x < \infty$, $0 < y < b$ and $0 < z < h$, by assuming the irrotational motion of the homogeneous, incompressible and inviscid fluid, the potential flow theory can be applied to model the fluid behavior. Accordingly, the oscillatory liquid flow in the fluid region is described by using the velocity potential, where due to the conservation of energy the velocity potential must satisfy the Laplace equation as:

$$\nabla^2\phi(x,y,z,t) = \phi_{,xx} + \phi_{,yy} + \phi_{,zz} = 0 \tag{1a}$$

Herein $\phi(x,y,z,t)$ is the velocity potential of the fluid and t is time. The velocity potential is related to three fluid velocity components (i.e. u,v,w) in the reference Cartesian coordinate system (i.e. xyz) as:

$$u = \phi_{,x},\ v = \phi_{,y},\ w = \phi_{,z} \tag{1b}$$

Due to the presence of rigid walls at two ends of the channel width, the fluid velocity in the direction normal to the walls is zero:

$$\text{At } y = 0: \qquad \phi_{,y} = 0 \tag{2}$$

$$\text{At } y = b: \qquad \phi_{,y} = 0 \tag{3}$$

The linearized boundary conditions at the fluid free surface and the seabed can be expressed as [14]:

$$\text{At } z = 0: \qquad \phi_{,t} + g\eta_s = 0 \tag{4a}$$

$$\phi_{,z} = \eta_{s,t} \tag{4b}$$

$$\text{At } z = -h: \qquad \phi_{,t} + \frac{P_p}{\rho} + g\eta_p = 0 \tag{5a}$$

$$\phi_{,z} = \eta_{p,t} \tag{5b}$$

where g is the gravitational acceleration, ρ is the fluid density, $P_p$is the fluid pressure applied on the plate surface, $\eta_p(x,y,t)$ and $\eta_s(x,y,t)$ are the plate's mid-plane displacement and the fluid free surface (i.e. $z=0$) displacement in z direction, respectively. Eqs. (4a) and (4b) can be combined and expressed as a single boundary condition as:

$$\text{At } z=0: \qquad \phi_{,tt}+g\phi_{,z}=0 \tag{5c}$$

The plate deformation in Eqs. (5a) and (5b) is the solution of following differential equation for a Kirchhoff plate:

$$At\ z=-h: \qquad D\nabla_{xy}^4\eta_p+\rho_p d\,\eta_{p,tt}+k^*\eta_p+c^*\eta_{p,t}-\rho\left(\phi_{,t}+g\eta_p\right)=0 \tag{6}$$

Where $D=Ed^3/\left(12(1-\nu^2)\right)$ is the flexural rigidity of the plate (E is the Young's modulus of plate and ν is its poison's ratio), ρ_p is the plate density, and c^* and k^* are the damping and stiffness coefficients of the viscoelastic foundation, respectively. It is important to note that the unsteady hydrodynamic pressure on the plate is obtained from Eq. (5a) as $P_p=\rho\left(\phi_{,t}+g\eta_p\right)$ and substituted in Eq. (6). The boundary conditions at $y=0$ and $y=b$ are also specified depending on type of the support considered for the plate. For instance, the simply supported boundary conditions impose $\eta_p(x,y=0,t)=0$, $\eta_p(x,y=b,t)=0$, $\eta_{p,yy}(x,y=0,t)=0$ and $\eta_{p,yy}(x,y=b,t)=0$.

In order to solve the boundary value problem for $\phi(x,y,z,t)$, which is specified in Eq. (1a) with the boundary conditions denoted in Eqs. (2), (3), (5b) and (5c), the normal mode method is utilized and a harmonic response (i.e. a function of time through a factor $e^{-i\omega t}$ where ω is the incident wave frequency and $i=\sqrt{-1}$) for the governing equation is sought. Correspondingly, we assume that the fluid disturbances due to the interaction between waves and deformable plate are small enough to utilize the superposition principle and express the velocity potential function as the summation of two sub-components; i.e. diffraction potential (ϕ_s) and radiation potential(ϕ_b), as:

$$\phi=\phi_s+\phi_b \tag{7}$$

The diffraction potential describes the velocity potential due to the incident wave plus the fluid scattered field by the plate at rest, while the radiation potential is generated due to the flexible plate oscillations. Therefore, each of the components in Eq. (7) must satisfy the Laplace differential equation in the whole fluid region:

$$\nabla^2\phi_b=0 \tag{8a}$$

$$\nabla^2\phi_s=0 \tag{8b}$$

The boundary conditions (2), (3), (5b) and (5c) can also rearranged for each mode as:

$$\text{At } y=0 \qquad \phi_{b,y}=0 \tag{9a}$$

$$\text{At } y=b \qquad \phi_{b,y}=0 \tag{9b}$$

$$\text{At } z=0 \qquad \phi_b=0 \tag{9c}$$

$$\text{At } z = -h \qquad \phi_{b,z} = \eta_{p,t} \tag{9d}$$

and:

$$\text{At } y = 0 \qquad \phi_{s,y} = 0 \tag{10a}$$

$$\text{At } y = b \qquad \phi_{s,y} = 0 \tag{10b}$$

$$\text{At } z = 0 \qquad -\omega^2\phi_s + g\left(\phi_{s,z} + \phi_{b,z}\right) = 0 \tag{10c}$$

$$\text{At } z = -h \qquad \phi_{s,z} = 0 \tag{10d}$$

Thus, the general form of velocity potentials for the radiation and diffraction modes can be assumed as:

$$\phi_b(x,y,z,t) = e^{i(kx-\omega t)} \sum_{m=0}^{M} a_{bm} \cos\left(\frac{m\pi}{b} y\right) \left(e^{A_m(z-h)} + q_{bm} e^{-A_m(z+h)}\right) \tag{11}$$

$$\phi_s(x,y,z,t) = e^{i(kx-\omega t)} \sum_{m=0}^{M} a_{sm} \cos\left(\frac{m\pi}{b} y\right) \left(e^{A_m z} + q_{sm} e^{-A_m z}\right) \tag{12}$$

where m is the normal mode number, a_{bm} and a_{sm} are the amplitudes of the corresponding modes. Upon substituting Eq. (11) into Eq. (8a) (or Eq. (12) into Eq. (8b)), $A_m$can be obtained as:

$$A_m = \sqrt{k^2 + \frac{m^2\pi^2}{b^2}} \tag{13}$$

Moreover, from Eqs. (9c) and (10d), we can obtain:

$$q_{bm} = -1 \tag{14}$$

$$q_{sm} = e^{-2A_m h} \tag{15}$$

Therefore, the radiation and diffraction modes of the velocity potential are expressed as:

$$\phi_b(x,y,z,t) = e^{i(kx-\omega t)} \sum_{m=0}^{M} a_{bm} \cos\left(\frac{m\pi}{b} y\right) \left(e^{A_m(z-h)} - e^{-A_m(z+h)}\right) \tag{16}$$

$$\phi_s = e^{i(kx-\omega t)} \sum_{m=0}^{M} a_{sm} \cos\left(\frac{m\pi}{b} y\right) \left(e^{A_m z} + e^{-A_m(2h+z)}\right) \tag{17}$$

The modal expansion technique can be utilized in a similar manner to express the general harmonic form of the vertical displacement for the fluid free surface (i.e. $z = 0$) as the following:

$$\eta_s(x,y,t) = e^{i(kx-\omega t)} \sum_{m=0}^{M} L_m \cos\left(\frac{m\pi}{b} y\right) \tag{18}$$

where L_m is the amplitude corresponding to the m^{th} mode in the harmonic response. In order to obtain the ratio between the amplitudes of velocity potential response in the fluid domain

(a_{bm} and a_{sm}) and free surface displacement (L_m), by recalling Eqs. (4b) and (7), $\eta_{s,t} = \phi_{,z} = \phi_{s,z} + \phi_{b,z}$ can be used in Eq. (10c) to obtain:

$$\text{At } z = 0 \qquad \eta_{s,t} = \frac{\omega^2}{g}\phi_s \tag{19}$$

Inserting Eqs. (17) and (18) into Eq. (19) yields:

$$a_{sm} = \frac{-igL_m}{\omega(1 + e^{-2A_m h})} \tag{20}$$

Subsequently, substituting a_{sm} from Eq. (20) into Eq. (17) and using the outcome and Eq. (16) in Eq. (10c) leads to:

$$a_{bm} = \frac{-ige^{A_m h}L_m}{2\omega}\left(\frac{\omega^2}{A_m g} - \tanh(A_m h)\right) \tag{21}$$

The superposition principle can be similarly utilized to derive the general semi-analytical solution of Eq. (6) as:

$$\eta_p(x, y, t) = e^{i(kx-\omega t)} \sum_{m=0}^{M} C_m Y_m(y) \tag{22}$$

Where C_m is the amplitude of the mth normal mode for the plate in y direction, and $Y_m(y)$ is the normalized (non-dimensional) mth mode shape of the plate wave propagating in y direction and it has to satisfy the boundary conditions in $y = 0$ and $y = b$. The general form of $Y_m(y)$ can be specified as:

$$Y_m(y) = \frac{Q_1 \cos(\beta_m y) + Q_2 \sin(\beta_m y) + Q_3 \cosh(\beta_m y) + Q_4 \sinh(\beta_m y)}{\sqrt{{Q_1}^2 + {Q_2}^2 + {Q_3}^2 + {Q_4}^2}} \tag{23}$$

where Q_1-Q_4 are the constants of the plate normal mode shape in y-direction. For instance, the simply-supported supports impose the following boundary conditions at $y = 0$ and $y = b$ for $Y_m(y)$:

$$Y_m(0) = 0\,, \quad Y_m''(0) = 0\,, \quad Y_m(b) = 0\,, \quad Y_m''(b) = 0 \tag{24}$$

By applying these conditions on Eq. (23), we can obtain $\beta_m = (m + 1)\pi/b$ and the following form for $Y_m(y)$:

$$Y_m(y) = \sin\left(\frac{(m + 1)\pi}{b} y\right) \tag{25}$$

By inserting Eqs. (16), (17) and (22) into Eq. (6), one obtains:

$$\sum_{m=0}^{M}\Big\{D\big[C_mY_m^{(4)}(y)-2C_mk^2Y_m''(y)+k^4C_mY_m(y)\big]-\rho_p d\omega^2C_mY_m(y)+k^*C_mY_m(y) - i\omega c^*C_mY_m(y)-\rho gC_mY_m(y)\Big\} + \sum_{m=0}^{M} i\rho\omega\left[a_{sm}\cos\left(\frac{m\pi}{b}y\right)(2e^{-A_mh})+a_{bm}\cos\left(\frac{m\pi}{b}y\right)(e^{-2A_mh}-1)\right]=0 \tag{26}$$

Also, substituting Eqs. (16) and (22) into the Eq. (9d) leads to:

$$\sum_{m=0}^{M} a_{bm}A_m\cos\left(\frac{m\pi}{b}y\right)(1+e^{-2A_mh})=-i\sum_{m=0}^{M}\omega\, C_mY_m(y) \tag{27}$$

Making use of the amplitude relations from Eqs. (20) and (21), multiplying both sides of Eqs. (17) and (18) by $\cos\left(\frac{n\pi}{b}y\right)$ (where $n=0,1,\dots,M$), and integrating over the plate width (i.e. $0<y<b$), one may obtain:

$$\begin{aligned}&\sum_{m=0}^{M}C_m\int_0^b\Big\{D\big[Y_m^{(4)}(y)-2k^2Y_m''(y)+k^4Y_m(y)\big]+k^*Y_m(y)-\rho gY_m(y)\Big\}cos(\frac{n\pi}{b}y)dy\\ &-\rho_p d\omega^2\sum_{m=0}^{M}C_m\int_0^b Y_m(y)\,cos\left(\frac{n\pi}{b}y\right)dy\\ &-i\omega c^*\sum_{m=0}^{M}C_m\int_0^b Y_m(y)\,cos\left(\frac{n\pi}{b}y\right)dy\\ &+\rho\omega\sum_{m=0}^{M}\left[\frac{2L_mg}{\omega(1+e^{-2A_mh})}e^{-A_mh}\right.\\ &\left.+\frac{L_mge^{A_mh}}{2\omega}\left(\frac{\omega^2}{A_mg}-tanh(A_mh)\right)(e^{-2A_mh}-1)\right]\int_0^b cos\left(\frac{m\pi}{b}y\right)cos\left(\frac{n\pi}{b}y\right)dy\\ &=0\quad \text{where} n=0,1,\dots,M\end{aligned} \tag{28-a}$$

$$\begin{aligned}&\sum_{m=0}^{M}L_m(\omega^2\,cosh(A_mh)-A_mg\,sinh(A_mh))\int_0^b cos\left(\frac{m\pi}{b}y\right)cos\left(\frac{n\pi}{b}y\right)dy\\ &=\omega^2\sum_{m=0}^{M}C_m\int_0^b Y_m(y)\,cos\left(\frac{n\pi}{b}y\right)dy\ \text{where}\ n=0,1,\dots,M\end{aligned} \tag{29-a}$$

Eqs. (28-a) and (29-a) can be expressed in terms of the dimensionless parameters as the followings:

$$\begin{aligned}&\sum_{m=0}^{M}C_m\int_0^b\left\{\varepsilon h^4\big[Y_m^{(4)}(y)-2k^2Y_m''(y)+k^4Y_m(y)\big]+\left(\frac{1}{\gamma}-1\right)Y_m(y)\right\}\cos(\frac{n\pi}{b}y)dy\\ &-R\Omega^2\sum_{m=0}^{M}C_m\int_0^b Y_m(y)\cos\left(\frac{n\pi}{b}y\right)dy-i\Omega\zeta\sum_{m=0}^{M}C_m\int_0^b Y_m(y)\cos\left(\frac{n\pi}{b}y\right)dy\\ &+\sum_{m=0}^{M}L_m\left[\frac{1}{\cosh(\mu_m)}\right.\\ &\left.-\left(\frac{\Omega^2}{\mu_m}-\tanh(\mu_m)\right)\sinh(\mu_m)\right]\int_0^b\cos\left(\frac{m\pi}{b}y\right)\cos\left(\frac{n\pi}{b}y\right)dy=0\quad \text{where} n\\ &=0,1,\dots,M\end{aligned} \tag{28-b}$$

$$\sum_{m=0}^{M} L_m(\Omega^2\, cosh(\mu_m) - \mu_m\, sinh(\mu_m)) \int_0^b cos\left(\frac{m\pi}{b}y\right) cos\left(\frac{n\pi}{b}y\right) dy = \Omega^2 \sum_{m=0}^{M} C_m \int_0^b Y_m(y)\, cos\left(\frac{n\pi}{b}y\right) dy \text{ where } n = 0,1,\dots,M \tag{29-b}$$

where the dimensionless parameters are specified as:

$$\Omega = \omega\sqrt{\frac{h}{g}}, \qquad \gamma = \frac{\rho g}{k^*}, \qquad \varepsilon = \frac{D}{\rho g h^4}, \qquad \zeta = \frac{c^*}{\rho\sqrt{gh}}, \qquad R = \frac{\rho_p d}{\rho h}$$
$$\tau = t\sqrt{\frac{g}{h}}, \qquad \mu_m = \sqrt{(\mu_x)^2 + \left(\mu_y\right)^2}, \qquad \mu_x = kh, \qquad \mu_y = \frac{m\pi h}{b} \tag{30}$$

Herein Ω is the non-dimensional frequency, μ_x is the shallowness parameter, γ is the restoring force coefficient, ε is the non-dimensional flexural rigidity, ζ is the non-dimensional damping ratio and R is the mass ratio. Expanding Eqs. (28-b) and (29-b) and rewriting them in the matrix form yields:

$$\Omega^2\mathbf{M}\cdot\mathbf{L} + \Omega\mathbf{D}\cdot\mathbf{L} + \mathbf{K}\cdot\mathbf{L} = \mathbf{0} \tag{31}$$

Where $\mathbf{M} \in \mathbb{R}^{(2M+2)\times(2M+2)}$ is the mass matrix, $\mathbf{D} \in \mathbb{R}^{(2M+2)\times(2M+2)}$ is the damping matrix, $\mathbf{K} \in \mathbb{R}^{(2M+2)\times(2M+2)}$ is the stiffness matrix, $\mathbf{0} \in \mathbb{R}^{2M+2}$ is the zero vector, $\mathbf{L} \in \mathbb{R}^{2M+2}$ is the (unknown) normal modes amplitude vector and they are expressed as:

$$\mathbf{M} = \begin{bmatrix}\mathbf{M}_{11} & \mathbf{M}_{12}\\ \mathbf{M}_{21} & \mathbf{M}_{22}\end{bmatrix}$$
$$\mathbf{D} = \begin{bmatrix}\mathbf{0} & \mathbf{0}\\ \mathbf{0} & \mathbf{D}_{22}\end{bmatrix}$$
$$\mathbf{K} = \begin{bmatrix}\mathbf{K}_{11} & \mathbf{0}\\ \mathbf{K}_{21} & \mathbf{K}_{22}\end{bmatrix} \tag{32}$$
$$\mathbf{L}^T = \{L_0, L_1, \cdots, L_{M-1}, L_M, C_0, C_1, \cdots, C_{M-1}, C_M\}$$

Where $\mathbf{0} \in \mathbb{R}^{(M+1)\times(M+1)}$ is the zero matrix and the components of sub-matrices $\mathbf{M}_{11}$,$\mathbf{M}_{12}$,$\mathbf{M}_{21}$,$\mathbf{M}_{22}$,$\mathbf{D}_{22}$,$\mathbf{K}_{11}$,$\mathbf{K}_{21}$,$\mathbf{K}_{22} \in \mathbb{R}^{(M+1)\times(M+1)}$ can be identified as:

$$\mathbf{M}_{11}(n,m) = \begin{cases} b\cosh(\mu_m) & \text{for } n = m = 0\\ \dfrac{b\cosh(\mu_m)}{2} & \text{for } n = m \neq 0\\ 0 & \text{for } n \neq m\end{cases} \tag{33a}$$

$$\mathbf{M}_{12}(n,m) = -\int_0^b Y_m(y)\cos\left(\frac{n\pi}{b}y\right) dy \tag{33b}$$

$$\mathbf{M}_{21}(n,m) = \begin{cases} \dfrac{-b\sinh(\mu_m)}{\mu_m} & \text{for } n = m = 0\\ \dfrac{-b\sinh(\mu_m)}{2\mu_m} & \text{for } n = m \neq 0\\ 0 & \text{for } n \neq m\end{cases} \tag{33c}$$

$$\mathbf{M}_{22}(n,m) = -R\int_0^b Y_m(y)\cos\left(\frac{n\pi}{b}y\right)dy \tag{33d}$$

$$\mathbf{D}_{22}(n,m) = -i\zeta\int_0^b Y_m(y)\cos\left(\frac{n\pi}{b}y\right)dy \tag{33e}$$

$$\mathbf{K}_{11}(n,m) = \begin{cases} -\mu_m b\sinh(\mu_m) & \text{for } n=m=0 \\ \dfrac{-\mu_m b\sinh(\mu_m)}{2} & \text{for } n=m\neq 0 \\ 0 & \text{for } n\neq m \end{cases} \tag{33f}$$

$$\mathbf{K}_{21}(n,m) = \begin{cases} b\left[\tanh(\mu_m)\sinh(\mu_m)+\dfrac{1}{\cosh(\mu_m)}\right] & \text{for } n=m=0 \\ \dfrac{b}{2}\left[\tanh(\mu_m)\sinh(\mu_m)+\dfrac{1}{\cosh(\mu_m)}\right] & \text{for } n=m\neq 0 \\ 0 & \text{for } n\neq m \end{cases} \tag{33g}$$

$$\mathbf{K}_{22}(n,m) = \int_0^b \left\{\varepsilon h^4\left[Y_m^{(4)}(y) - 2k^2Y_m''(y) + k^4Y_m(y)\right] + \left(\frac{1}{\gamma}-1\right)Y_m(y)\right\}\cos(\frac{n\pi}{b}y)dy \tag{33h}$$

Now, after calculating the required matrices in Eq. (31) from Eqs. (33a)-(33h), the necessary and sufficient conditions for the presence of a non-trivial solution in terms of **L** can be expressed as the following eigenvalue problem:

$$\det\left(\Omega^2\mathbf{M} + \Omega\mathbf{D} + \mathbf{K}\right) = 0 \tag{34}$$

Eq. (34) is the dispersion relation for the wave propagation through the plate in contact with the fluid due to the fluid free surface incident wave moving along the *x*-axis. Using the dispersion equation, one may obtain the relationship between the angular frequency and wavenumber of the propagating bending wave in the plate. The corresponding shapes of the normal modes are the eigenvectors of Eq. (34), while the general form of $Y_m(y)$ for the simply supported boundary conditions at $y=0$ and $y=b$is obtained in Eq. (25), for two other well-known types of boundary conditions (sliding-sliding and clamped-clamped) can be obtained as the followings.

Sliding-Sliding

At sliding boundaries, the slope and shear force are zero. Hence, the boundary conditions can be stated as:

$$Y_m'(0)=0,\quad Y_m'(b)=0,\quad Y_m'''(0)=0,\quad Y_m'''(b)=0 \tag{35}$$

Substituting these conditions into Eq. (23) gives the transverse mode shape function as:

$$Y_m(y) = \cos\left(\frac{m\pi}{b}y\right) \tag{36}$$

Clamped-Clamped

At clamped boundaries, the displacement and slope are zero. In other words:

$$Y_m(0)=0,\quad Y_m(b)=0,\quad Y_m'(0)=0,\quad Y_m'(b)=0 \tag{37}$$

By inserting the above mentioned conditions into Eq. (23), one can obtain:

$$Y_m(y) = \cos(\beta_m y) - \cosh(\beta_m y) - \frac{\cos(\beta_m b)-\cosh(\beta_m b)}{\sin(\beta_m b)-sinh(\beta_m b)}(sin(\beta_m y) - sinh(\beta_m y)) \tag{38}$$

where the first ten values of β_m have been listed in Table 1 [19].

Table 1
The first ten values of $\beta_m b$ for the plate with clamped-clamped boundary conditions.

m	1	2	3	4	5	6	7	8	9	10
$\beta_m b$	4.7300	7.8532	10.9956	14.1372	17.2788	20.4204	23.5619	26.7035	29.8451	32.9867

In order to verify the present solution, we can obtain the dynamic response of a similar problem but for a simplified case. A similar problem with sliding-sliding boundary conditions has been presented in [14] using rather a different solution method where only the contribution of the first mode has been considered in the system dynamic response (i.e. $m = 0$). Using a similar method and substituting Eq. (36) into the Eqs. (28) and (29) and letting $m = 0$, the following equations can be obtained:

$$L_0(\Omega^2 \cosh(\mu_0) - \mu_0 \sinh(\mu_0)) - i\Omega^2 C_0 = 0 \tag{39}$$

$$C_0\left\{\varepsilon\mu_0^4 + \left(\frac{1}{\gamma} - 1\right) - R\Omega^2 - i\Omega\zeta\right\} + iL_0\left[\left(\frac{\Omega^2}{\mu_0} - \tanh(\mu_0)\right)\sinh(\mu_0) - \frac{1}{\cosh(\mu_0)}\right] = 0 \tag{40}$$

By simplifying these equations, the dispersion relation can be stated as:

$$\begin{aligned}\Omega_0^4(R\gamma\mu_0 + \gamma\tanh(\mu_0)) + i\Omega_0^3\mu_0\zeta\gamma - \Omega_0^2(R\mu_0^2\gamma\tanh(\mu_0) + \varepsilon\mu_0^5\gamma + \mu_0) - i\Omega_0\zeta\mu_0^2\gamma\tanh(\mu_0)\\ + \mu_0^2(1-\gamma)\tanh(\mu_0) + \varepsilon\mu_0^6\gamma\tanh(\mu_0) = 0\end{aligned} \tag{41}$$

Eq. (41) is identical with the dispersion relation expressed in [14]. Likewise, by neglecting the flexural rigidity and also the plate mass, the dispersion relation presented in [13] can be extracted:

$$\Omega_0^4\gamma\tanh(\mu_0) + i\Omega_0^3\mu_0\zeta\gamma - \Omega_0^2\mu_0 - i\Omega_0\zeta\mu_0^2\gamma\tanh(\mu_0) + \mu_0^2(1-\gamma)\tanh(\mu_0) = 0 \tag{42}$$

4. Results

4.1. Validation

To validate the results, the numerical results of the governing equations proposed in this study evaluated with results published in the literature.
In Fig. 3, the frequency response of system by solving equation (42) is shown. The frequency response of system by considering assumptions of [13] is exactly the same as those presented in Fig. 3 of [13].

By solving Eq. (34) (dispersion relation), four values will be obtained for the frequency; two values for the plate mode and two values for the surface mode. These frequency values are in the form $\pm\Omega_r - i\Omega_i$ where Ω_r and Ω_i are the positive real numbers. It is worth noting that once the real part of frequency is negative, it shows that waves move along $-x$ direction. In this study, it assumed that waves move along $+x$ direction [20].

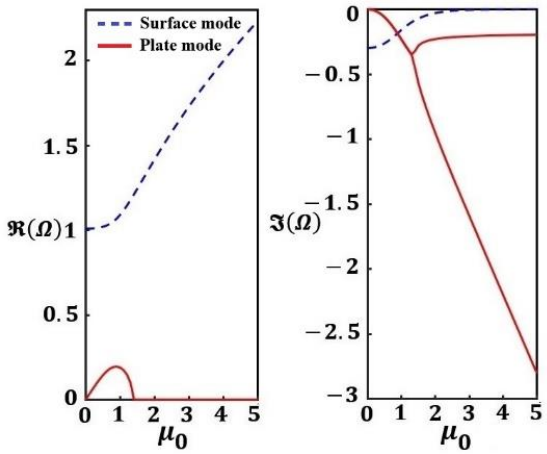

Fig. 3. Real and Imaginary parts of system frequency response of Eq. (42).

First of all, we will check the convergence test. In Fig. 5, the convergence test for the first four frequencies has been presented for the plate with simple-simple end conditions. The results have been obtained by solving Eq. (27) for M=8 and M=9. It should be noted that the vertical and horizontal axes indicates the imaginary and real parts of the frequency, respectively. From here on and based on these results, the number of term in the series expansion, M, will be taken equal to 9 in all the following examples.

Likewise, the first mode shapes of the plate and surface have been depicted in Fig. 6 for different boundary conditions (B.C.). The following dimensionless parameters have been considered to obtain Fig. 6:

$$R = 0.01, \quad \gamma = 0.9, \quad \varepsilon = 0.01, \quad \zeta = 0.6, \quad \mu = 5 \tag{63}$$

Unless mentioned otherwise, the above values have been taken to obtain the results.

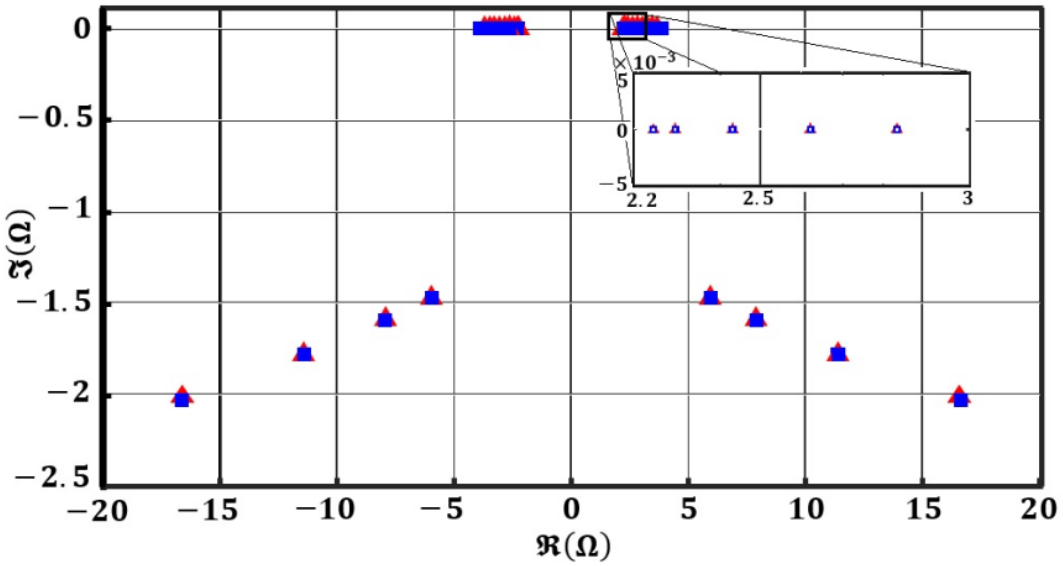

Fig.5. Convergence test for the frequency response.

(Blue rectangle: M=8, Red triangle: M=9)

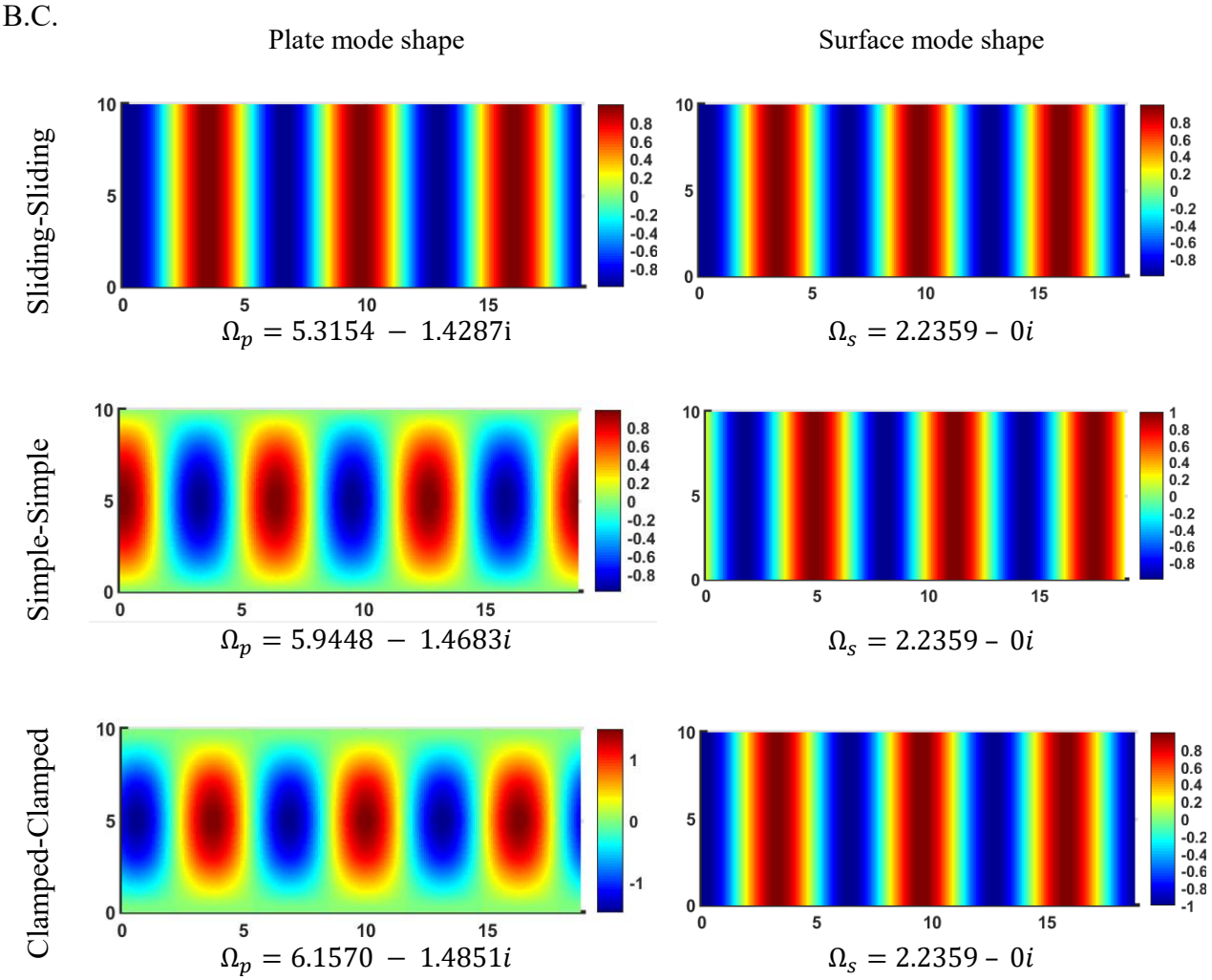

Fig. 6. First mode shape of the plate and surface for different boundary conditions.

A close inspection reveals that the frequency and mode shape of the surface are almost the same for all boundary conditions at the large values of μ. Therefore, the boundary conditions of the plate have almost no effect on the frequency and mode shape of the surface at deep channel. In addition, the frequency of the plate with clamped and sliding boundary conditions has the higher and lower values, respectively.

4.2. Results

In the subsequent sections, the effects of boundary conditions, plate's rigidity and mass, damping ratio, restoring force of viscoelastic bed and wave number on the frequencies are investigated. It should be note that in all the following figures, the plate and surface modes have been distinguished by solid and dashed lines, respectively.

4.2.1. Effect of boundary conditions

In Fig. 7, the real and imaginary parts of the fundamental frequency for the plate and surface are displayed for different boundary conditions.

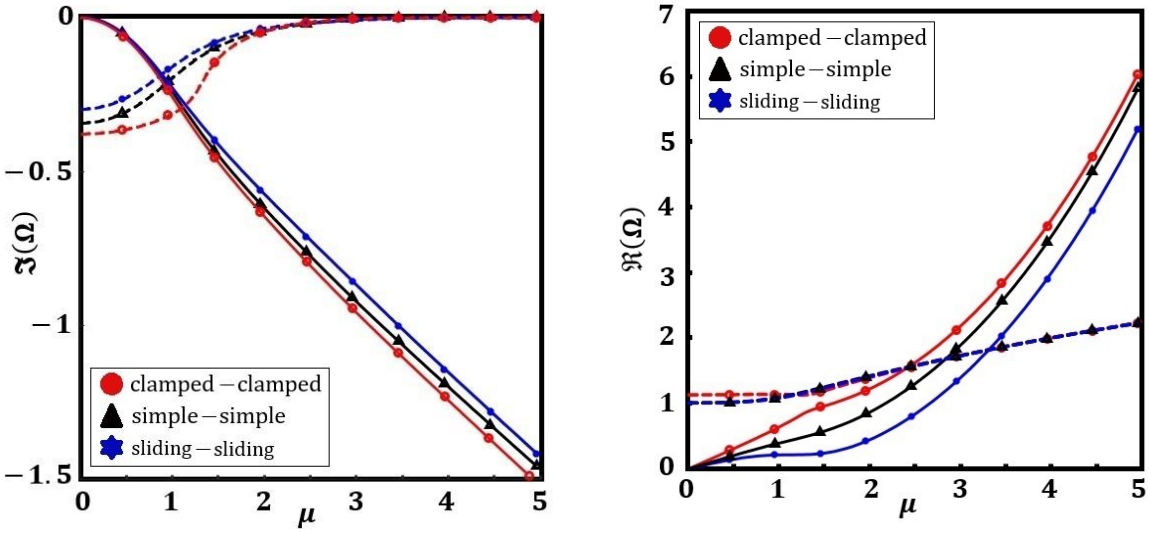

a) Imaginary Part

b) Real Part

Fig.7. Fundamental frequency of the plate and surface for different boundary conditions.

It can be seen that for the plate mode, the sliding-sliding boundary condition has the lowest value of the real part of frequency and the clamped-clamped boundary condition has the highest value. In addition, the absolute value of the imaginary part of frequency for the sliding-sliding boundary condition and the clamped-clamped boundary condition are the highest and the lowest value, respectively. In other words, in the equal conditions, the plate with clamped-clamped boundary conditions attenuates waves faster.

It is clear that the shallowness is proportional to the inverse of wavelength. By inspecting the surface modes, one can deduce that for the shorter waves (larger values of μ), the real and imaginary parts of the surface mode are almost the same for all boundary conditions. While for the long waves, the clamped-clamped boundary conditions damps faster than the other two boundary conditions.

4.2.2. Effect of plate rigidity

Plate rigidity plays an important role in the dynamic response. In Fig. 8, its effects on the plate and surface modes has been investigated in which the real and imaginary parts of the frequency have been depicted for three values of ε. It should be mentioned that unless mentioned otherwise the simple-simple end conditions have been considered for all subsequent results.

By increasing the plate rigidity, the real part of the frequency increases while its imaginary part decreases. It means that a plate with more flexural rigidity attenuate waves faster. However, for the surface mode the effect of rigidity of plate is not very significant, especially for the real part of the frequency.

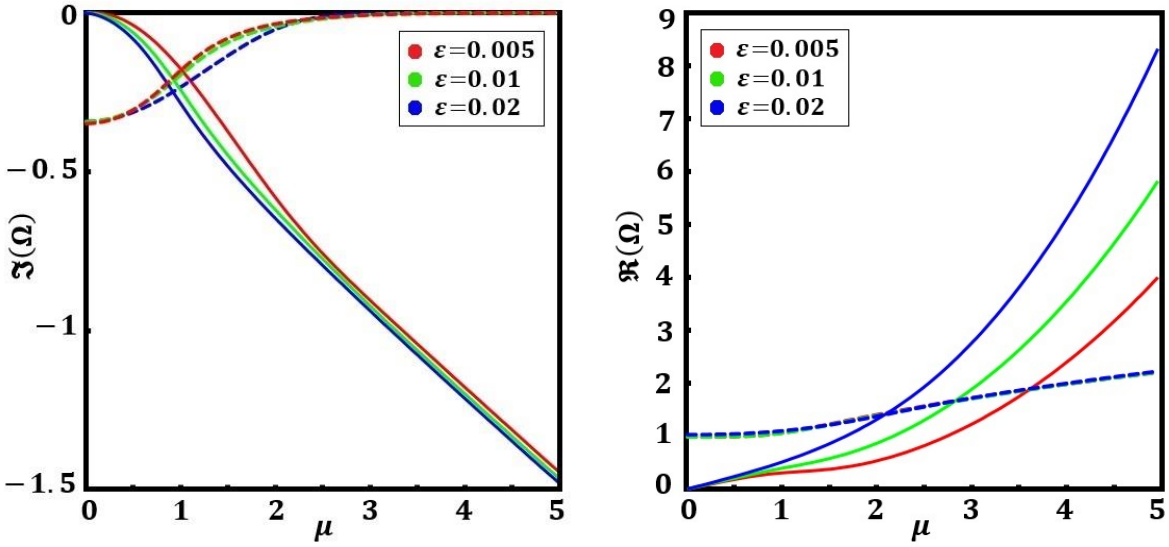

a) Imaginary Part b) Real Part

Fig. 8. The effect of plate rigidity on the fundamental frequency of the system for the plate with simple-simple boundary conditions.

4.2.3. Effect of plate mass

The plate mass is another parameter that can influence the frequency of the system. In Fig. 9, the fundamental mode of the plate with simple end conditions has been calculated for three different values of the plate mass ratio.

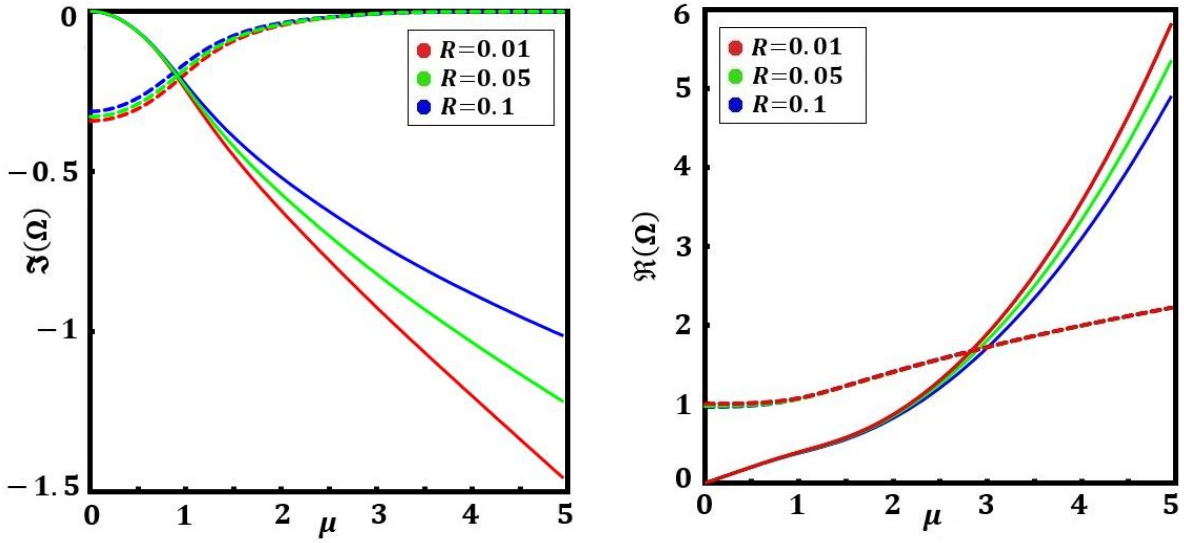

a) Imaginary Part b) Real Part

Fig. 9. The effect of plate mass on the fundamental frequency of the system for the plate

with simple-simple boundary conditions.

As it is expected, the effect of plate's mass on the surface mode is negligible. There is a little changes in imaginary part of frequency of surface mode only for the long waves which means that the surface mode damps later by increasing the plate mass. For the plate mode, by increasing plate mass, the real part of the frequency decreases but the imaginary part of frequency increases. It means that a plate with higher density damps slower and oscillates with longer period.

4.2.4. Effect of damping ratio

Dampers are responsible to attenuate waves by simulate viscous behavior of muddy seabed. Therefore, it is crucial to investigate the influence of damping ratio on the frequency response. The imaginary and real parts of the fundamental frequency versus shallowness parameter for three different values of damping ratio have been depicted in Fig. 10.

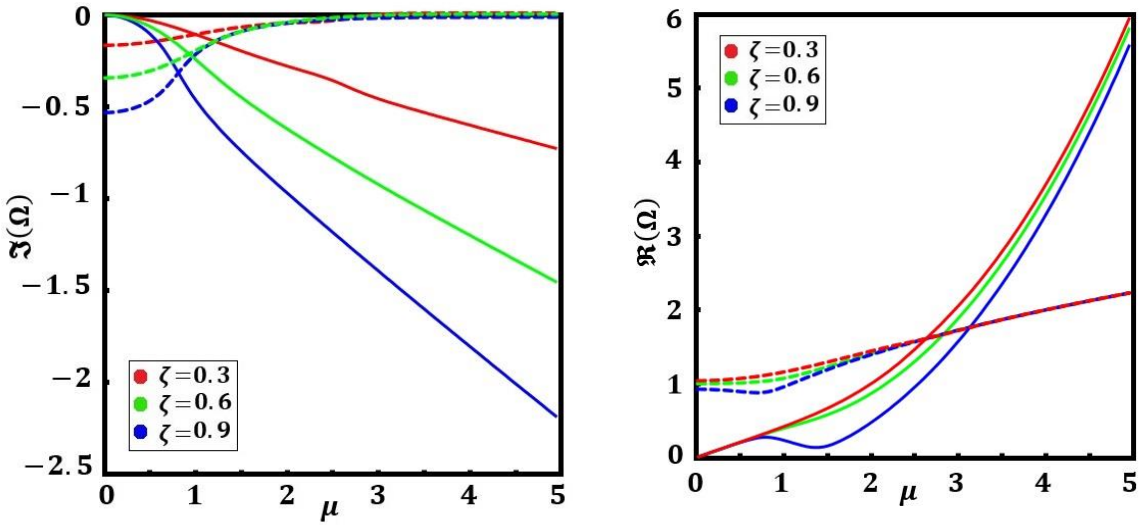

a) Imaginary Part b) Real Part

Fig. 10. The effect of damping ratio on the fundamental frequency of the system for the plate with simple-simple boundary conditions.

As can be seen for the surface mode, the damping ratio can only affect the wave propagation frequencies of the longer wave lengths. For long wave lengths and by increasing the damping ratio, the real part and the imaginary part of frequency decrease.

For the plate mode, by increasing the damping ratio, the real and imaginary parts of the frequency decrease at all wave lengths.

4.2.5. Effect of restoring force

Referred to Eq. (30), the restoring force coefficient is proportional to the inverse of spring's stiffness constant. In Fig. 11, the influence of the restoring force coefficient on the fundamental frequency of the plate and surface has been investigated.

For the short waves, the effect of restoring force on the real and imaginary parts of the surface mode is negligible. The notable effect of stiffness is on the real part of plate frequency in which by increasing the stiffness, the plate oscillates with a shorter period.

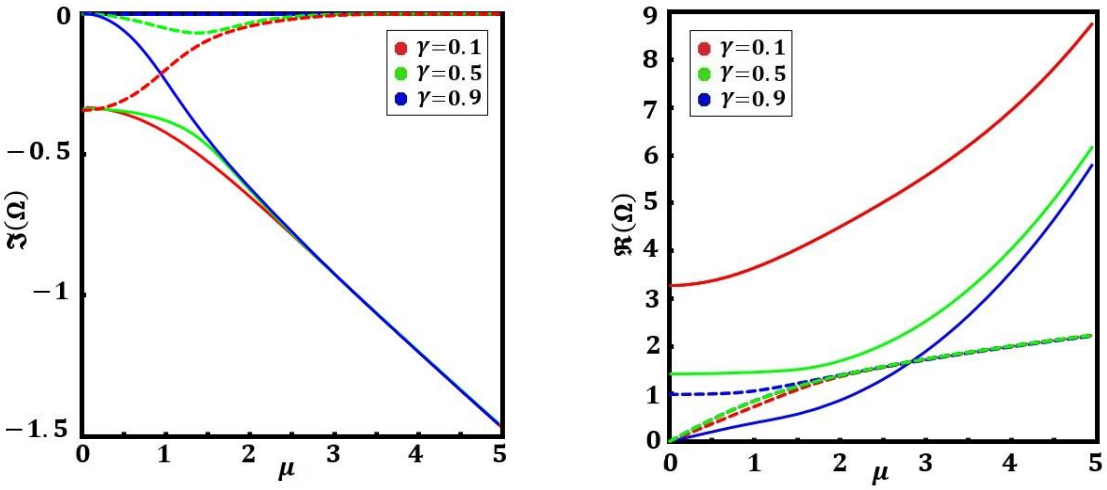

a) Imaginary Part b) Real Part

Fig. 11. The effect of restoring force on the fundamental frequency of the system for the plate with simple-simple boundary conditions.

4.2.6. Effect of different modes

The effect of the wave number on the first four transverse modes of the system for the plate with simple-simple boundary conditions has been plotted in Fig. 12.

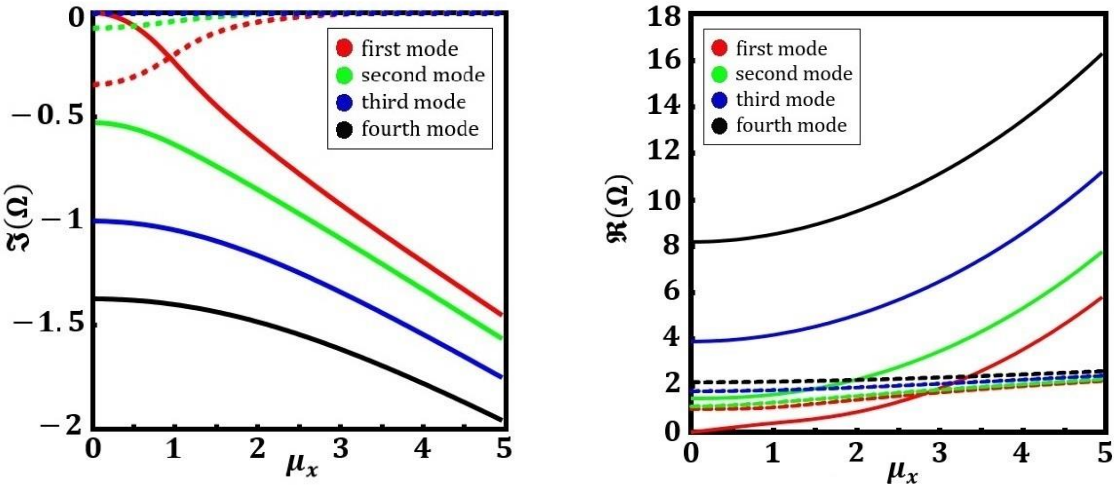

a) Imaginary Part b) Real Part

Fig.12. The effect of wave number on the different modes of the system for the plate with simple-simple boundary conditions.

By inspecting the imaginary part of the plate frequency, one can say that by decreasing the wave length the rate of the damping will increase. For the plate mode, the real part of frequency increases by increasing mode of system, which means the plate oscillates with less period in higher modes. In addition, the plate in higher modes damps earlier. However, for the surface mode, increasing mode of system causes the increase of real part of frequency and imaginary part of frequency. However, for the real part of the surface mode, the increasing rate is not the same as those observed for the plate.

5. Conclusions

In this paper, the muddy seabed has been modeled as a viscoelastic foundation which is placed under a thin plate located at the bottom of a channel to investigate the vibrational behavior of the system. Arbitrary boundary conditions have been considered for the plate in the width direction. Unlike previous studies, the fluid-structure interaction system by considering the flexural rigidity and mass of the plate is analyzed in three dimensions in the present study. A new solution method has been presented to obtain the solution. It is shown that the system has four frequency responses i.e. two responses for plate mode and two responses for surface mode.

The results are summarized as follows:

1. Under different boundary conditions, the submerged plate with clamped-clamped boundary condition has lower period and attenuates waves faster. In other words, plate with higher flexible rigidity oscillates with less period attenuate the waves faster.

2. The plate with less mass attenuate the waves faster. The result showed that the effect of mass of the submerged plate is important and it should be considered in the mathematical modeling of the system.

3. As expected, waves attenuate faster by increasing the damping ratio.

4. By increasing the stiffness of springs, the plate oscillates with lower period.

5. By comparing different transverse modes under the same conditions, it is observed that in higher modes the plate oscillates with less period and attenuate faster.

Funding

The first and third authors acknowledge the funding support of Babol Noshirvani University of Technology through Grant program No. BNUT/944130042/95.

Conflicts of Interest

The authors declare no conflict of interest.

Authors Contribution Statement

Arman Asaiean: Conceptualization; Methodology; Data curation; Formal analysis; Software; Writing – original draft, Maryam Abedi: Conceptualization; Supervision; Methodology; Writing

– review & editing, Ramazan-Ali Jafari-Talookolaei: Project administration; Supervision; Writing – review & editing, Mostafa Attar: Supervision; Writing – review & editing.

References

[1] Creel L. Ripple effects: population and coastal regions. Population Reference Bureau Washington, DC; 2003.

[2] Gade HG. Effects of a nonrigid, impermeable bottom on plane surface waves in shallow water. J Mar Res 1958;16:61–81.

[3] Holland KT, Vinzon SB, Calliari LJ. A field study of coastal dynamics on a muddy coast offshore of Cassino beach, Brazil. Cont Shelf Res 2009;29:503–14. doi:10.1016/j.csr.2008.09.023.

[4] Elgar S, Raubenheimer B. Wave dissipation by muddy seafloors. Geophys Res Lett 2008;35:n/a-n/a. doi:10.1029/2008GL033245.

[5] Silvester R. Headland defense of coasts, Coastal Engineering Proceedings 1976;1.

[6] Mac Pherson H, Kurup PG. Wave damping at the Kerala mudbanks 1981.

[7] Sheremet A, Stone GW. Observations of nearshore wave dissipation over muddy sea beds. J Geophys Res Ocean 2003;108.

[8] Macpherson H. The attenuation of water waves over a non-rigid bed. J Fluid Mech 1980;97:721. doi:10.1017/S0022112080002777.

[9] Dalrymple RA, Liu PLF. Waves over soft muds: a two-layer fluid model. J Phys Oceanogr 1978;8:1121–31.

[10] Alam M-R, Liu Y, Yue DKP. Waves due to an oscillating and translating disturbance in a two-layer density-stratified fluid. J Eng Math 2009;65:179–200.

[11] Ko-Fei L, Mei CC. Long waves in shallow water over a layer of bingham-plastic fluid-mud—I. Physical aspects. Int J Eng Sci 1993;31:125–44. doi:10.1016/0020-7225(93)90070-B.

[12] Alam M-R. A Flexible Seafloor Carpet for High-Performance Wave Energy Extraction. Vol. 4 Offshore Geotech. Ronald W. Yeung Honor. Symp. Offshore Sh. Hydrodyn., American Society of Mechanical Engineers; 2012, p. 839–46. doi:10.1115/OMAE2012-84034.

[13] Alam M-R. Nonlinear analysis of an actuated seafloor-mounted carpet for a high-performance wave energy extraction. Proc R Soc A Math Phys Eng Sci 2012;468:3153–71. doi:10.1098/rspa.2012.0193.

[14] Asaeian A, Jafari-Talookolaei R-A, Abedi M, Attar M. Dynamic investigation of wave energy absorber plate located on the bottom of a channel. Modares Mech Eng 2018;18:361–9.

[15] Sahoo T, Yip TL, Chwang AT. Scattering of surface waves by a semi-infinite floating elastic plate. Phys Fluids 2001;13:3215–22. doi:10.1063/1.1408294.

[16] Mondal R, Sahoo T. Wave structure interaction problems for two-layer fluids in three dimensions. Wave Motion 2012;49:501–24. doi:10.1016/j.wavemoti.2012.02.002.

[17] Havelock TH. LIX. Forced surface-waves on water. London, Edinburgh, Dublin Philos Mag J Sci 1929;8:569–76. doi:10.1080/14786441008564913.

[18] Evans D V, Porter R. Wave scattering by narrow cracks in ice sheets floating on water of finite depth. J Fluid Mech 2003;484:143.

[19] Rao SS. Vibration of continuous systems. vol. 464. Wiley Online Library; 2007.

[20] Ball FK. Energy transfer between external and internal gravity waves. J Fluid Mech 1964;19:465.